ACOUSTO-OPTIC PHENOMENA IN CRYSTALS WITH STRONG ANISOTROPY OF OPTIC AND ELASTIC PROPERTIES

V.B.Voloshinov
Department of Physics, M.V.Lomonosov Moscow State University, Moscow, RUSSIA
volosh@osc162.phys.msu.ru

Abstract

The paper examines regular trends of acousto-optic interactions taking place in crystals possessing strong anisotropy of optic and elastic properties. The major attention is devoted to analysis of light diffraction in media with large birefringence, i.e. with big difference $\Delta n = n_e - n_o$ between the refraction indexes of ordinary n_o and extraordinary n_e polarized optical beams. The analysis is also concentrated on peculiarities of light and ultrasound interaction in anisotropic materials that possess strong anisotropy of elastic properties. Single crystals of paratellurite (TeO_2), tellurium (Te), calomel (Hg_2Cl_2), mercury bromide (Hg_2Br_2) and mercury iodide (Hg_2I_2) were investigated owing to the large birefringence and due to the extremely wide obliquity angles $\Psi > 50^0$ between phase and group velocities of ultrasound. The paper considers regular trends of light diffraction in the anisotropic media and examines possible applications of new diffraction phenomena in novel modifications of acousto-optic instruments.

Introduction

The paper is devoted to investigation of light diffraction by ultrasound propagating in crystalline media possessing strong anisotropy of optic and elastic properties. It is known that materials with the anisotropy of their physical properties have successfully been used in acousto-optic instruments of light beam control [1,2]. Many modifications of acousto-optic devices applying the diffraction have been designed and applied in modern Optics, Spectroscopy, Optical Information Processing and Laser Technology [3,4]. However, new acousto-optic crystalline materials were synthesized in recent times. It is reasonable to expect that the new materials that possess extremely strong anisotropy of physical properties will be considered as candidates for the application in novel modifications of acousto-optic devices such as filters, deflectors and modulators [1-4].

The major attention during the present investigation is devoted to analysis of light diffraction in the optically anisotropic crystals possessing extraordinary large birefringence. In particular, the acousto-optic interaction is examined in the crystals with the difference $\Delta n = n_e - n_o$ between the indexes of refraction of the extraordinary n_e and ordinary n_o polarized optical beams as big as the refractive indexes themselves, i.e. $\Delta n \sim n_o$. It should be noted that efficient acousto-optic crystals have been grown with the relative birefringence b of the order $b = \Delta n / n_o = 0.3 - 0.4$ [1,5].

In this paper, the crystals characterized by the large birefringence $b > 0.3$ such as tellurium (Te), calomel (Hg_2Cl_2), mercury bromide (Hg_2Br_2) and mercury iodide (Hg_2I_2) are examined with the goals of application in acousto-optic instruments [1-5]. It is likely that novel types of modulators, deflectors and tunable acousto-optic filters (AOTFs) will be developed on base of the unique birefringent materials. Moreover, it may be expected that the new devices, in many aspects, will be superior to the existing acousto-optic systems of light beams control.

It was noticed that many of the new acousto-optic materials were characterized not only by the strong anisotropy of their optical properties but also by the strong anisotropy of their elastic properties [4-7]. It is known that the elastic anisotropy manifests itself in the extremely large obliquity angles Ψ between phase and group velocities of ultrasound [4]. The acoustic "walkoff" angle Ψ evaluated between the acoustic wave vector and the Poynting vector may appear in the crystals as large as dozens of degrees. For example, the obliquity angle in the single crystal of tellurium is exceeding $\Psi > 50^0$ while the walkoff angle in calomel, mercury bromide and mercury iodide is about $\Psi = 70^0$ [6,7]. As for the commonly used tellurium dioxide single crystals, they are also of undoubted interest for the applications because TeO_2 is characterized by the acoustic obliquity angles up to $\Psi = 74^0$ [7]. The carried out investigation proves that the unusual propagation of the elastic waves in these media results in new effects that may be observed during the interactions of light and ultrasound [6-9].

The regimes of the acousto-optic interactions existing only in the materials possessing the strong optic and elastic anisotropy are examined in the presentation. Many of the interactions have not yet been realized in experiments. On the other hand, there are diffraction regimes that are well known in Acousto-Optics and that have been successfully used in acousto-optic devices [3,7-10]. The paper describes modifications of acousto-optic instruments that may be designed on base of the new effects existing in the optically and elastically anisotropic materials.

Optical anisotropy of crystals

Optical anisotropy of a uniaxial crystal is characterized by the value of birefringence Δn equal to the difference between the refractive indexes of two optical modes that propagate in a medium transparent to radiation. The anisotropy of a crystalline material is also described by a surface of optic wave vectors or a wave surface. In a uniaxial crystal, the wave surface is represented by a sphere and an ellipsoid surrounding the sphere and touching it at two points along the direction of the optical axis z [1].

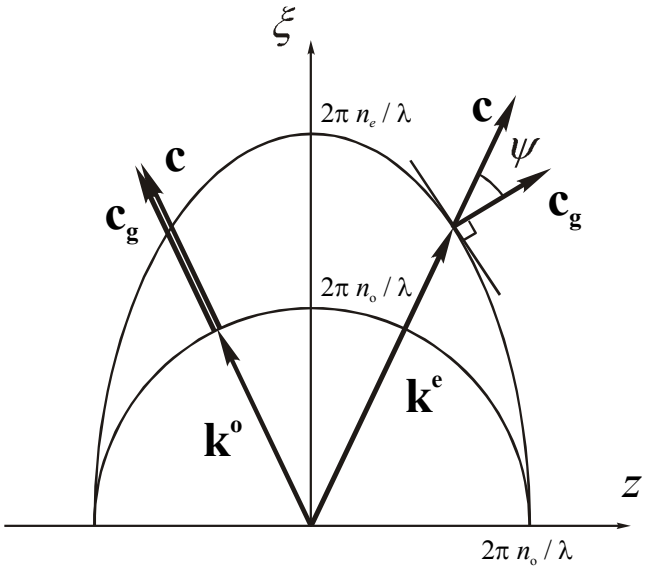

Figure 1: Wave surface of a positive optic crystal

Cross-section of the wave surface of a positive ($n_e > n_o$) optical crystal is schematically shown in figure 1. It may be seen in the figure that the lengths of the optic wave vectors $\mathbf{k}^o$ and $\mathbf{k}^e$ are equal to $k = 2\pi n / \lambda$ where λ is the wavelength of light and n is the refractive index of either ordinary or extraordinary polarized optical wave. It is known that a normal installed, at an optic wave vector end, orthogonally to a wave surface shows direction of group velocity $\mathbf{c_g}$ of light. On the other hand, phase velocity vector $\mathbf{c}$ is parallel to the vector $\mathbf{k}^o$.

It is known that the phase $\mathbf{c}$ and group $\mathbf{c_g}$ velocity vectors of light are equal to each other and coincide in a glass material. As for a crystal, they coincide in the case of the ordinary polarized rays. These waves in figure 1 are illustrated by the wave vector $\mathbf{k^o}$. On the other hand, data in figure 1 demonstrate that the extraordinary polarized optical beam with the wave vector $\mathbf{k}^e$ is propagating with the optic obliquity angle ψ between the phase velocity vector $\mathbf{c}$ and the group velocity vector $\mathbf{c_g}$.

It should be noted that the drawing in figure 1 only illustrates the general trend because the difference in the lengths of the wave vectors $\mathbf{k}^o$ and $\mathbf{k}^e$ in figure 1 is exaggerated compared to a real crystal. Analysis confirms that, in the majority of optical materials known so far in Acousto-Optics, the relative birefringence does not exceed the magnitude $b = \Delta n / n_o = 0.1$ [1]. For example, the crystal of quartz $\alpha - SiO_2$ is characterized by the relative birefringence $b = 0.006$ while the crystals of lithium niobate $LiNbO_3$ and paratellurite TeO_2 possess correspondingly the birefringence coefficients equal to $b = 0.04$ and $b = 0.07$.

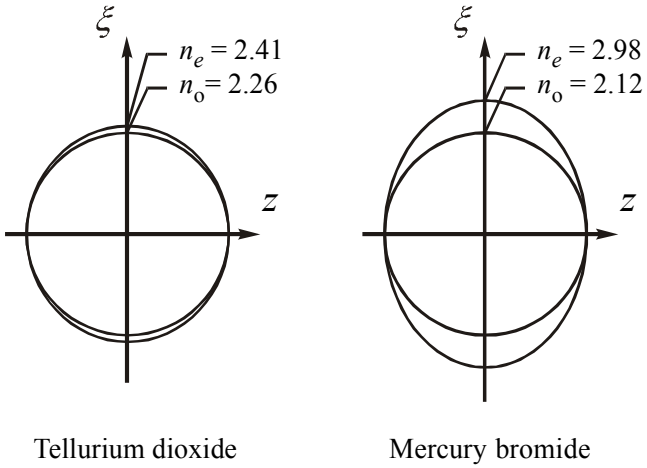

Figure 2: Wave surfaces of paratellurite and mercury bromide

It was mentioned that such materials as tellurium, calomel and mercury bromide demonstrate much larger birefringence, e.g. of the order $b \geq 0.3$. Figure 2 shows the wave surfaces of paratellurite and mercury bromide plotted in real scale with respect to the indexes of refraction. It is easy to conclude that the optic obliquity angle in the case of Hg_2Br_2 is larger than that of tellurium dioxide. The laws of Optics prove that the higher the birefringence the larger the angle between the phase and group velocity of light in a crystal [1].

The value of the optic obliquity angle in a uniaxial crystal may be calculated by means of the expression

$$\psi = \arctan\left[(n_e / n_o)^2 \tan\varphi\right] - \varphi \qquad (1)$$

where φ is the angle of propagation in the crystal measured with respect to the axis ξ orthogonal to the optical axis z. Calculation demonstrates that if the refraction indexes at the wavelength of light $\lambda = 633$ nm in paratellurite are equal to $n_e = 2.41$ and $n_o = 2.26$ then the maximum optical obliquity

angle in TeO_2 is limited to $\psi < 4^0$. This obliquity angle is observed along the direction with $\varphi \approx 45^0$.

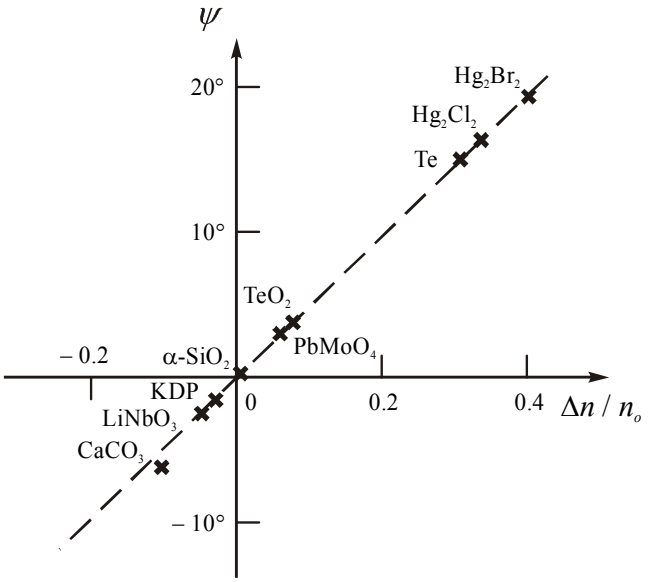

Figure 3: Optic walkoff angle in crystals

However, a similar optical walkoff angle in the single crystal of calomel with the refractive indexes in the visible light $n_e = 2.62$ and $n_o = 1.96$ occurs as large as $\psi \approx 16^0$. Data in figure 3 present results of calculation of the maximum optical obliquity angles ψ versus the relative birefringence $b = \Delta n / n_o$ in various crystalline materials. Positive values of the

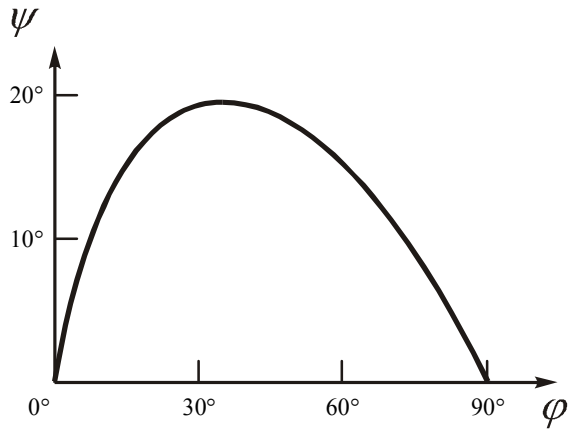

Figure 4: Optic obliquity angle of single crystal mercury bromide

relative birefringence in the figure correspond to the positive optical crystals with $n_e > n_o$ while the negative crystals are represented in figure 3 by the coefficients $b < 0$. It may be seen in the figure that the materials that possess the extremely wide optical obliquity angles $\psi > 15^0$ are mercury bromide, mercury chloride and tellurium.

Results of calculation of the optic obliquity angle in Hg_2Br_2 versus a direction of propagation in the crystal are plotted in figure 4. The angular dependence was calculated by means of equation (1) at $n_e = 2.975$ and $n_o = 2.121$ typical of the material in the visible light. It is seen in figure 4 that the maximum optical obliquity angle in mercury bromide is extremely large $\psi \approx 20^0$. This walkoff angle is observed along the direction of light propagation at the angle $\varphi = 35^0$ corresponding to the polar angle 55^0 evaluated relatively to the optical axis.

Application of materials with large birefringence in acousto-optic imaging instruments

The carried out analysis proves that peculiar types of interactions between light and sound exist in the crystals with the large birefringence. For example, it was found that, during the interaction, energy flows of

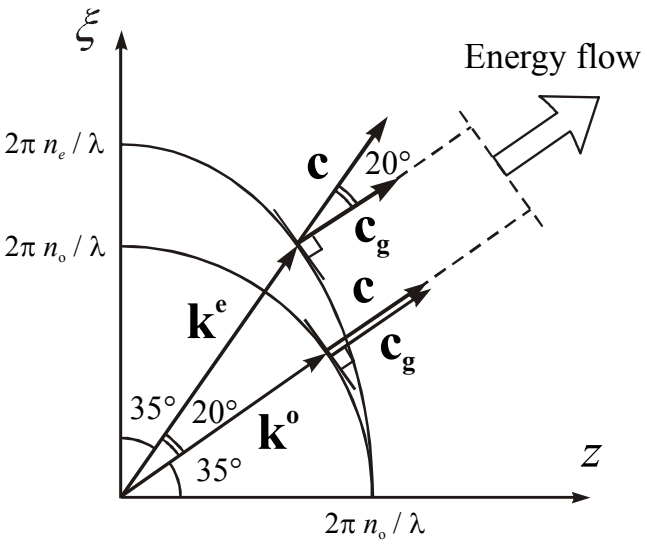

Figure 5: Optic wave vectors in mercury bromide

all three or at least two of the interacting optic and acoustic beams may occur collinear. On the contrary, wave vectors of these rays remain principally not collinear forming different from zero angles between each other. It is also possible to observe another type of acousto-optic interaction in the crystals when the wave vectors are directed collinear while the energy flows of the interacting rays propagate at angles with respect to each other. It should be mentioned that these interactions are of interest not only to the fundamental knowledge but also to applied sciences. New acousto-optic instruments may be developed on base of these peculiar diffraction regimes.

An example of such instrument is described in the paper. In particular, an imaging acousto-optic filter with improved operation parameters may be

developed if one selects the materials with large birefringence as the medium of light and sound interaction. Mercury bromide is just one of the crystals that are promising for the application.

As mentioned, mercury bromide possesses one of the largest optic obliquity angle among other birefringent materials. Data in figure 4 and figure 5 confirm this statement. Analysis demonstrates that if an extraordinary polarized optical beam is sent in Hg_2Br_2 at the angle $\varphi = 35^0$ relatively to the axis ξ then the group velocity $\mathbf{c_g}$ of the extraordinary polarized light is directed at the angle $\varphi = 55^0$ with respect to the axis ξ . The obliquity angle in this case is equal to $\psi = 20^0$, as illustrated in figure 4. On the other hand, if an ordinary polarized beam is propagating in the crystal at the angle $\varphi = 55^0$ relatively to ξ then the wave vectors $\mathbf{k^o}$ and $\mathbf{k^e}$ of the two beams are separated in space by the angle $\Delta\theta \approx 20^0$, as proved in figure 5.

In spite of the wide angle $\Delta\theta$ between the two optic wave vectors in figure 5, the group velocity vectors $\mathbf{c_g}$ of the two optical beams occur collinear, i.e. parallel to each other. The condition of parallel group velocities of the two beams in the crystal indicates that tangents to the wave surfaces at the ends of the optical wave vectors in figure 5 are also parallel to each other.

The above presented analysis so far was based only on consideration of the optic beams. However, if an acoustic wave with a specially chosen frequency is generated in the crystal in such a manner that the acoustic wave vector **K** connects the ends of the two optical wave vectors in figure 5 then Bragg phase matching condition is satisfied in the crystal during the diffraction [1-4]. It means that efficient acousto-optic anisotropic interaction may take place in the birefringent material. This interaction is described by the traditional vector triangle

$$\mathbf{k_i^o} + \mathbf{K} = \mathbf{k_d^e} , \qquad (2)$$

where the wave vectors $\mathbf{k_i^o}$ and $\mathbf{k_d^e}$ represent the incident ordinary polarized and the diffracted extraordinary polarized optical radiation. This vector triangle in mercury bromide is shown in figure 6. As seen, the direction of the acoustic vector **K** in figure 6 is determined by the angle α evaluated relatively to the axis ξ. This is just the angle between the optical axis of the crystal and the acoustic wave front.

It is known in Acousto-Optics, that the condition of parallel tangents to wave surfaces at ends of interacting optical wave vectors corresponds to the non-critical or wide-angle acousto-optic interaction geometry [1-4,8]. This geometry is used in tunable acousto-optic filters (AOTFs) capable of processing of convergent optical beams and rays forming images. Therefore, the presented consideration proves the possibility to design a wide-angle imaging filter on base of single crystal mercury bromide. However, this is not the major advantage of the birefringent material. The analysis of the interaction geometry in Hg_2Br_2 reveals one more peculiarity of the diffraction that will be discussed below.

The characteristic feature of the diffraction in Hg_2Br_2 consists in the conclusion that the incident and the diffracted optical wave fronts in the crystal are separated by the angle $\Delta\theta$ as large as 20^0. Mutual orientation of the optical wave vectors in figures 5 and 6 prove this statement. It is known in that the spatial separation angle $\Delta\theta$ determines angular aperture of an imaging filter [3,8]. For example, the maximum value of the separation angle in paratellurite is limited to $\Delta\theta = 3.8^0$ in the

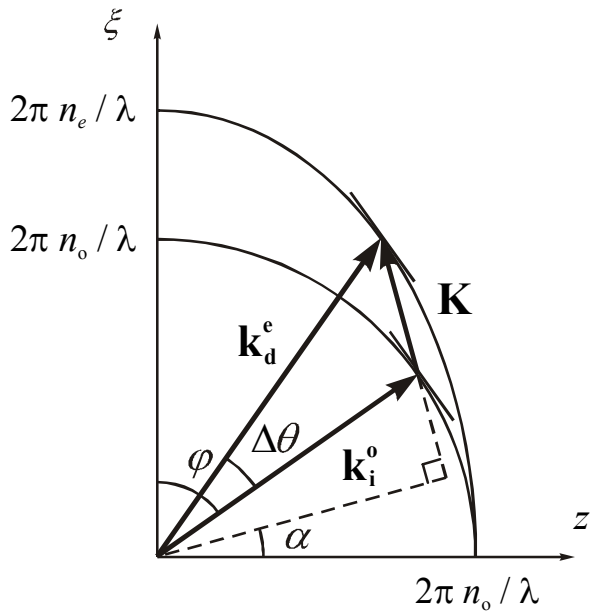

Figure 6: Wave vector diagram of interaction in mercury bromide

crystal resulting in the angular aperture about $\Delta\theta = 9^0$ in air [8]. As for mercury bromide, the presented analysis proves that the angular aperture of a filter fabricated on base of the crystal Hg_2Br_2 may be as wide as $\Delta\theta = 46^0$ because the aperture in air is approximately n_o = 2.12 times wider than in the material. Consequently, the filter shown in figure 7 will provide improvement in the angule apertures of the instrument to a factor of 5 relatively to the best modifications of the filters utilizing TeO_2 single crystals.

It should be mentioned that a filter with a wide angular aperture possesses the advantage of high

throughput as well as of convenience of adjustment and operation. Moreover, it may be proved that application of the filters with the wide apertures $\Delta\theta$ is accompanied by improvement in spatial resolution and, hence, optical quality of processed images.

The conclusion about the extremely wide angular aperture in mercury bromide is confirmed by the general expression demonstrating that the angle aperture of a tunable imaging filter is proportional to the birefringence value Δn of the applied material

$$\Delta\theta = (\Delta n / n_o) \cdot \sin^2\theta \cdot \cot\ (\theta - \alpha) \quad . \qquad (3)$$

According to the vector diagram in figure 6, the polar angle of light incidence θ in equation (5) is equal to $\theta = \pi/2 - \varphi$. As for the angle α, it determines the direction of the acoustic wave vector in the crystal, as mentioned. The carried out calculations prove that, in tellurium dioxide, the maximum angular aperture $\Delta\theta = 9^0$ of an AOTF in air is obtained in the crystal cut at $\alpha = 19^0$. In mercury bromide, the maximum aperture $\Delta\theta = 46^0$ is observed at the acoustic vector angle α a few degrees smaller than in TeO_2.

It was found that growth of the birefringence Δn is accompanied in the imaging AOTFs by improvement in spectral resolution. This advantage of the birefringent materials will be discussed in the following section of the paper.

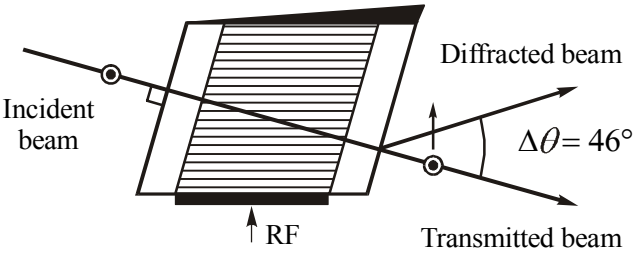

Figure 7: Acousto-optic cell of wide angle filter applying mercury bromide

Application of crystals with large birefringence in collinear and close to collinear AOTFs

The advantage of the large birefringence my be used in a collinear acousto-optic filter in which phase and group velocities of interacting beams are directed collinear to each other [1-4]. It is known that frequency of ultrasound f satisfying Bragg matching condition in a pure collinear regime of light diffraction is equal to

$$f = \Delta n\ V / \lambda \ , \qquad (4)$$

where V is phase velocity of ultrasound [1-5]. As seen in equation (4), selection of materials with the large birefringence Δn for filter application is accompanied by the evident growth of the acoustic frequency f . It means that the wavelength of ultrasound $\Lambda = V / f$ equal to a spatial period of acoustically induced diffraction grating in a crystal is decreasing with the frequency. That is why the spectral bandwidth of transmission $\Delta\lambda$ in a collinear AOTF becomes narrower with the growth of the birefringence if a total length of a crystal is fixed.

This improvement in the optical passband $\Delta\lambda$ and in the spectral resolution $R = \lambda / \Delta\lambda$ is illustrated by the known expression describing the spectral transmission bandwidth of a collinear AOTF

$$\Delta\lambda = 0.8\ \lambda^2 / \Delta n\ L \ . \qquad (5)$$

In the above expression, L is a length of the acousto-optic interaction usually equal to a size of a crystal [1-4].

A similar trend is typical of a close to collinear (quasi-collinear) acousto-optic filter [9-11]. It is evident that application of the crystals with large birefringence is accompanied in a quasi-collinear device by increase of the driving RF frequency f and by the corresponding shortening of the acoustic wavelength Λ. The growth of the frequency, so as in the collinear instruments, makes optical passband of the close to collinear instruments narrow. This conclusion is confirmed by the expression valid for the spectral bandwidth of a quasi-collinear filter

$$\Delta\lambda \approx \frac{0.8\ \lambda^2\ \sin(\theta + \alpha)}{\Delta n\ L \cdot \cos\Psi \cdot \sin^2\theta} \quad . \qquad (6)$$

In the above equation, Ψ is the acoustic obliquity angle, θ is the polar angle of light incidence and α is the angle determining direction of phase velocity of ultrasound.

As for the imaging devices applying the wide angle geometry of light and sound interaction, the spectral bandwidth of these acousto-optical instruments is equal to

$$\Delta\lambda \approx \frac{0.8\ \lambda^2\ \cos(\theta - \alpha)}{\Delta n\ L \cdot \sin^2\theta} \cdot [1 + \tan\Psi \cdot \tan(\theta - \alpha)] . \quad (7)$$

It may be seen in equations (6) and (7) that application in the filters of the materials with large birefringence is quite reasonable. In all examined classes of the AOTFs their passband $\Delta\lambda$ is decreasing with the growth of the difference Δn between the indexes of refraction of the extraordinary and ordinary polarized optical waves. In this respect,

mercury bromide, calomel and mercury iodide are about 4-5 times better than tellurium dioxide.

Advantages of application of the crystals possessing the large birefringence in the acousto-optic modulators and deflectors are not so evident and they will be discussed elsewhere. However, it is evident that the strong birefringence of crystals applied in the modulators and deflectors results at output of the instruments in larger angles $\Delta\theta$ between transmitted and diffracted optical beams. In general, it may improve signal-to-noise ratio and dynamic range of the acousto-optic devices. This advantage usually originates from lower levels of optical noise that arrives in a detector from zero order of diffraction.

Acousto-optic interactions in crystals with strong anisotropy of elastic properties

It is known that acoustic waves may propagate in paratellurite, calomel and in the other compounds of mercury with the acoustic obliquity angles as large as $\Psi \geq 70^0$ [4-7]. It was found that the anisotropy of the crystals influences on the process of light diffraction by ultrasound. For example, in the Raman-Nath and intermediate between Raman-Nath and Bragg regimes of light diffraction, the anisotropy results in asymmetry of distribution of light intensity over diffraction orders with positive and negative numbers [6]. In the Bragg regime the anisotropy influences on the diffracted light intensity and on the acoustic frequency bandwidths of interactions [6,7,11].

Presence in the crystals of the strong acoustic energy walkoff makes it possible to observe, in the elastically anisotropic media, interactions that may not be observed in isotropic media. For example, the interactions with collinear group velocities of the three interacting beams [2,3] or the close to collinear diffraction [9,10] may be mentioned in this context. It should be pointed out that these regimes of interaction have found applications in modern modifications of acousto-optic instruments, e.g. in the AOTFs intended for processing of optical signals in WDM waveguide communication lines [10].

It was noticed that propagation in the crystals of acoustic waves with the large angle Ψ between the phase and group velocity of ultrasound is accompanied by unusual reflection of the waves from a free boundary separating a crystal and vacuum [7,11]. This type of the reflection in XY plane of paratellurite is schematically shown in figure 8 where the incident and as much as two reflected acoustic waves may be recognized. As seen in the picture, the incident elastic energy, after the reflection from the bottom facet of the specimen, propagates approximately backwards with respect to the incident wave.

Recently it was proved that the angle Ω separating the incident and one of the reflected energy flows in paratellurite is be as narrow as a few

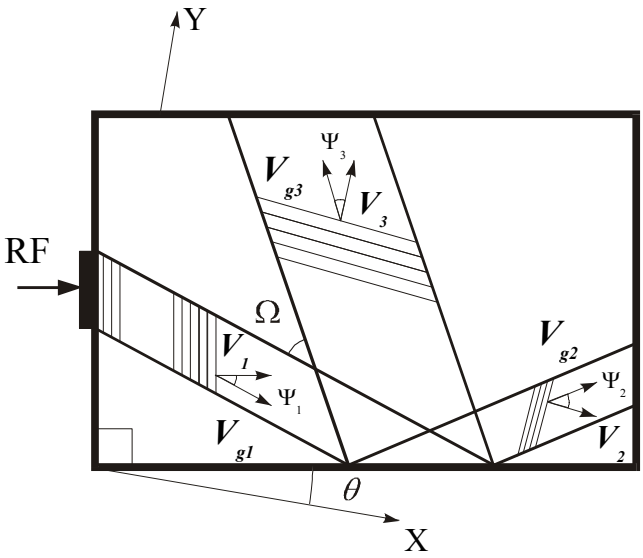

Figure 8: Acoustic reflection from a free boundary in tellurium dioxide

degrees. It was also found that this peculiar case of the acoustic reflection exists in the material in a wide variety of crystal cuts. Calculations confirm that the angle θ formed by the crystal boundary and the axis X of the material may be varied in the limits $3^0 < \theta < 23^0$ while the separation angle Ω remains limited to $\Omega < 10^0$.

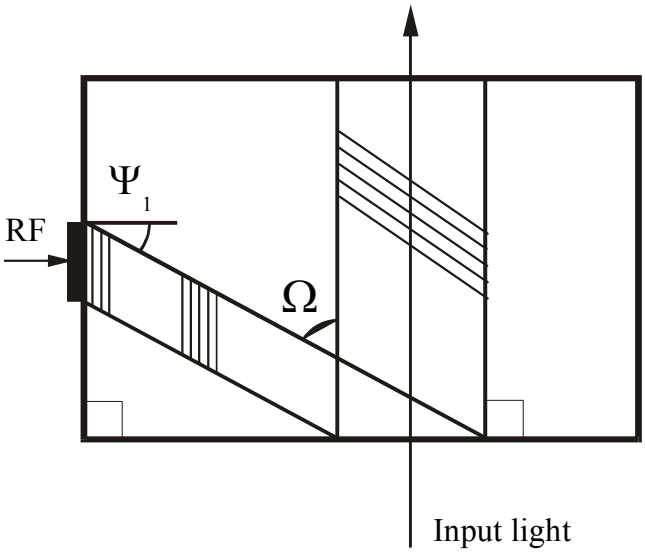

Figure 9. Acousto-optic cell with collinear interaction of beams

It is also possible that the reflected energy propagates in a cell strictly orthogonally to the border separating the crystal and vacuum. General view of the cell with collinear optic and acoustic energy flows

is presented in figure 9. In the predicted case of reflection, the acoustic obliquity angle Ψ_1 of the initial wave and the angle Ω of spatial separation of the incident and the reflected acoustic energy flows are coupled by the evident relation

$$\Omega = 90^0 - \Psi_1 \quad . \qquad (8)$$

It should be pointed out that all above described cases of acoustic propagation in the crystals with the strong elastic anisotropy may be used in novel modifications of acousto-optic devices.

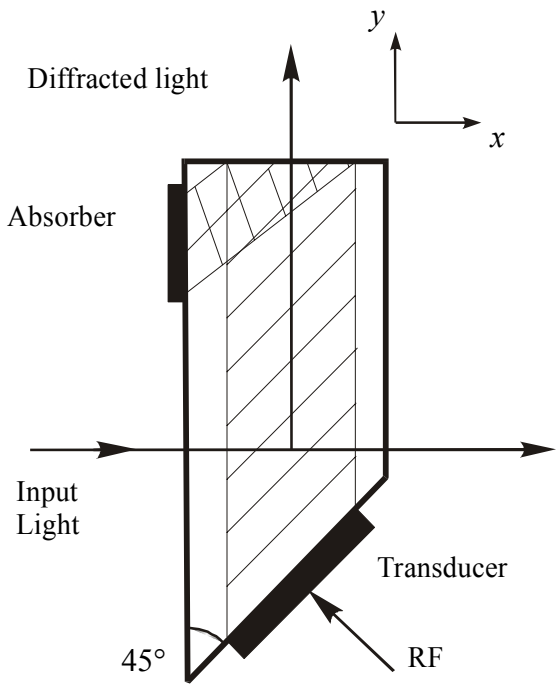

Figure 10: Mixed acousto-optic interaction in crystal with elastic energy walkoff

For example, the backward and the orthogonal acoustic reflection may be utilized in tunable acousto-optic filters with the collinear and quasi collinear interaction of beams [7,9-11].

In this paper, two new cases of the interactions not previously observed in Acousto-Optics are described. General scheme of one of the interactions is shown in figure 10. The interaction takes place in the cell shown in the picture. As seen, the acousto-optic cell is cut in form of a prism. Ultrasound propagates in the material with the acoustic obliquity angle equal to $\Psi = 45^0$, as illustrated in the figure. It means that the acoustic energy flow is directed along y axis. As for the optical wave, it is sent in the cell along x axis orthogonally to the borders of the acoustic column.

Wave vector diagram of the described regime of interaction is presented in figure 11. The diagram illustrates the condition of Bragg phase matching $\mathbf{k_i} + \mathbf{K} = \mathbf{k_d}$ in the cell. As seen in the figure, the wave vector of the incident optical beam $\mathbf{k_i}$ is directed along the axis x while the diffracted beam is represented by the wave vector $\mathbf{k_d}$ directed along the axis y.

The vector diagram proves that the diffracted beam in figure 11 is propagating orthogonally to the incident optical ray and, on the other hand, collinearly with the acoustic energy flow. It is clear that the collinear propagation of the diffracted light with the energy flow of ultrasound is provided by the elastic anisotropy of the crystal and by the special choice of the interaction geometry.

Analysis proves that two diffraction processes are simultaneously taking place in the cell shown in figure 10. One of these processes is a typical non-collinear diffraction. During this process, the incident optic

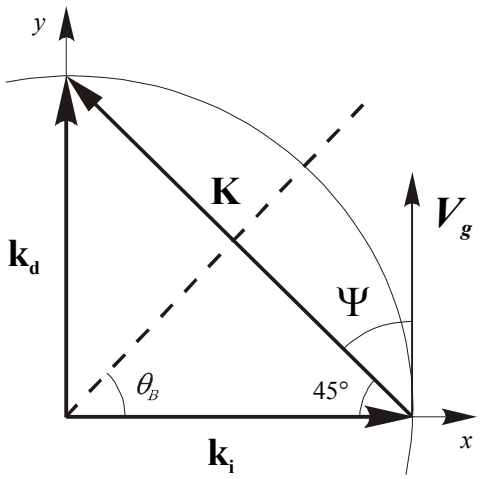

Figure 11: Wave vector diagram of mixed interaction

energy is diffracted by ultrasound so that intensity of the diffracted beam is growing along the axis x. On the contrary, intensity of the incident beam is vanishing along x because of scattering of the input optic energy to the diffracted beam.

Analysis of the interaction in figure 10 confirms that a collinear diffraction simultaneously takes place in the cell along the axis y. During the collinear interaction, the intensity of the diffracted beam occurs dependent on the distance inside the acoustic column covered by the diffracted light. This dependence originates form the back scattering of the diffracted energy to the zero diffraction order. Therefore, it may be predicted that the intensity of the diffracted beam is decreasing with the growth of the interaction length along the axis y. As a result of the mixed diffraction

in figure 10, the diffracted light intensity occurs dependent on both coordinates, i.e. x and y.

A modification of the examined interaction is shown in figure 12. It is seen in the figure that the incident optical beam propagates in the cell collinearly with the ultrasound in opposite direction with respect to the acoustic energy flow. Figure 12 proves that the diffracted beam is scattered by ultrasound orthogonally to the incident optical ray and to the borders of the acoustic column. As a result of the interaction, cross section of the diffracted ray occurs as large as the size of the crystal along the acoustic propagation. Consequently, intensity of the diffracted beam is dependent on the distance between the diffracted ray and the piezoelectric transducer.

It should be pointed out that the described regimes of interaction have not so far been observed in acousto-optic experiments. However, the new interactions are of undoubted interest to specialists due to the unusual character of the diffraction process taking place in a crystal. It is quite likely that these unknown regimes of the interaction will find applications in novel modifications of acousto-optic devices.

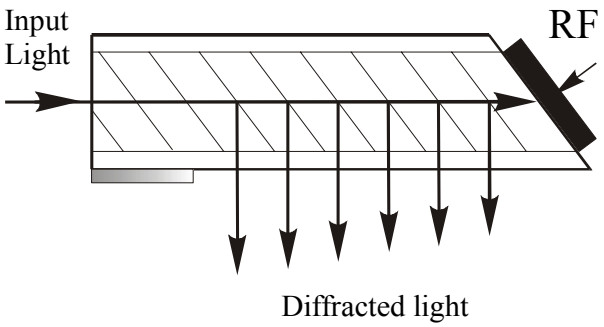

Figure 12: Acousto-optic cell with collinear interaction of beams

Conclusions

The carried out analysis demonstrates that diffraction of light by ultrasound in crystals possessing strong anisotropy of their optic and elastic properties differs from interactions in materials possessing moderate anisotropy. It is shown that large birefringence of a crystal results in a wide spatial separation of incident and diffracted optical beams at output of acousto-optic cells. It provides unique possibilities to design acousto-optic devices superior to the existing instruments of light beam control. Improvements in angular apertures, optical throughput, spatial resolution and signal-to-noise ratio seem quite likely in this case.

Application of crystals with the strong elastic anisotropy makes it possible to observe diffraction phenomena that so far are not known in Acousto-Optics. It is evident that new acousto-optic devices for modulation, scanning and filtering of optical radiation may be developed on base of the interactions existing only in the anisotropic crystalline materials.

Acknowledgement

The Russian Foundation for Basic Research, Grant N 02-07-90448, in part supported the research.

References

[1] A.Yariv and P.Yeh, Optical Waves in Crystals, Ed. John Wiley and Sons, New York, 1984.

[2] J.Xu and R.Stroud, Acousto-Optic Devices, Ed. John Wiley and Sons, New York, 1992.

[3] A.Goutzoulis and D.Pape, Design and Fabrication of Acousto-Optic Devices, Ed. Marcel Dekker Inc., New York, 1994.

[4] E.Dieulesaint and D.Royer, Ondes Elastiques dans les Solides, Ed. Mason, Paris, 1974.

[5] M.Gottlieb, A.Goutzoulis and N.Singh, "High-Performance Acousto-Optic Materials: Hg_2Cl_2 and $PbBr_2$", Optical Engineering, vol. 31, pp. 2110-2117, 1992.

[6] V.Voloshinov and O.Makarov, "Diffraction of Light by Ultrasound in Acoustically Anisotropic Medium", Proc. SPIE, vol. 3581, pp. 108-117, 1998.

[7] V.B.Voloshinov, "Application of Acousto-Optic Interactions in Anisotropic Media for Control of Light Radiation", Actes du 6^o Congres National Francias d'Acoustique, Lille, France, pp.283-288, 2002.

[8] V.B.Voloshinov and O.V.Mironov, "Wide Angle Acousto-Optic Filter for Middle Infrared Region of Spectrum", Optics and Spectroscopy, vol. 68, pp. 452-457, 1990.

[9] V.Voloshinov, "Close to Collinear Acousto-Optic Interaction in Paratellurite", Optical Engineering, vol. 31, pp. 2089-2094, 1992.

[10] J.Sapriel, D.Charissoux, V.Voloshinov and V.Molchanov, "Tunable Acousto-Optic Filters and Equalizers for WDM Applications", Journal of Lightwave Technology, vol. 20, pp.892-899, 2002.

[11] V.B.Voloshinov and N.V.Polikarpova, "Application of Acousto-Optic Interactions in Anisotropic Media for Control of Light Radiation", Acustica - Acta Acustica, vol. 89, 2003.